Title	Tuning magnetic properties, thermal stabilityandmicrostructure of NdFeB magnets with diffusing Pr-Znfilms
Author(s)	Jiajie Li, Xiangyun Huang, Liangliang Zeng, Bo Ouyang, Xiaoqiang Yu, Munan Yang, Zhenchen Zhong, Bin Yang and Rajdeep Singh Rawat
Source	*Journal of Materials Science & Technology, 41, 81-87*
Published by	Elsevier

Tuning magnetic properties, thermal stability and microstructure of NdFeB magnets with diffusing Pr-Zn films

Jiajie Li[1,2,3], Xiangyun Huang[1,2], Liangliang Zeng[1,2], Bo Ouyang[3], Xiaoqiang Yu[1], Munan Yang[1], Zhenchen Zhong[1], Bin Yang[2], Rajdeep Singh Rawat[3*]**

[1] Jiangxi Key Laboratory for Rare Earth Magnetic Materials and Devices (IREMMD), Jiangxi University of Science and Technology, Ganzhou, 341000, China

[2] School of Material Science and Engineering, Jiangxi University of Science and Technology, Ganzhou, 341000, China

[3] National Institute of Education, Nanyang Technological University, 637616, Singapore

Abstract

Grain boundary diffusion process (GBDP) serves as a promising approach in improving magnetic properties and thermal stability of NdFeB permanent magnets. Herein, non-heavy rare earth Pr-Zn films deposited on the magnet surface using DC-magnetron sputtering system are reported. The thermal stability and coercivity enhancement mechanism of Pr-Zn GBDP magnets are investigated systematically. The coercivity of Pr-Zn GBDP magnet was increased from 963.96 kA m^{-1} to 1317.14 kA m^{-1} without any remanence reduction. Notably, the demagnetization curve of Pr-Zn GBDP magnet still remained a high squareness ratio. The temperature coefficient of coercivity and anti-demagnetization ability of Pr-Zn GBDP magnet under high temperatures are improved after GBDP treatment. The well-optimized rare earth-rich (RE-rich) grain boundary phases and high effective anisotropy field of $(Nd,RE)_2Fe_{14}B$ magnetic hardening layers surrounding main grains are the key factors to impact the magnetic properties and thermal stability of NdFeB permanent magnets via GBDP treatment.

Keywords: NdFeB magnets, Magnetron sputtering, Pr-Zn films, Magnetic properties, Thermal stability

1. Introduction

NdFeB permanent magnet has drawn considerable attention due to its outstanding

* Corresponding author.
Email address: rajdeep.rawat@nie.edu.sg (R.S. Rawat).

magnetic properties from 1983 [1]. It gradually becomes indispensable part in many high-tech applications, including wind power [2], electric and hybrid vehicles [2], maglev trains [3] and intelligent robots [4], as well as in our daily life in the past thirty years. Continuous enhancement of such magnet performance has been devoted to meet the requirement of specific high-temperature applications. However, the actual operating temperature of NdFeB is relatively low because of the low Curie temperature (~ 312 ℃), leading to a rapid coercivity reduction under high temperatures. So far, the achieved coercivity is far below the theoretical value which is assumed as the anisotropy field of $Nd_2Fe_{14}B$ (~70 kOe) in Stoner-Wohlfarth model [5]. Herein, tremendous efforts have been made to improve the coercivity and thermal stability using different methods.

Substitution of heavy rare earth (HRE) Dy/Tb elements for Pr/Nd elements serves as an essential approach, to form the $(Pr/Nd,HRE)_2Fe_{14}B$ with relatively higher anisotropy field, which is named as single alloying method [6]. However, it may extremely reduce the saturation magnetization of $Nd_2Fe_{14}B$ owing to the anti-parallel magnetic moments between HRE and Fe atoms [7]. Another method is to introduce Dy/Pr-based alloys or inorganic compounds into NdFeB powders, called as dual alloying method [8]. But an apparent aggregation of RE-rich compounds or alloy phases at the triple junction RE-rich grain boundaries is harmful to the magnetic property improvement of the magnets. In addition, the scarcity of HRE resources on earth also limit their scalable usage.

Accordingly, GBDP technique recently becomes a promising alternative in preparation of high-performance magnets. Park et al [9] applied Dy metal coating on the surface of thin NdFeB sintered magnets to enhance the coercivity. Typically, HRE elements were covered onto NdFeB surface by different treatments, i.e. dip-coating [10,11,12], evaporation [13], melt-spun ribbons [14], magnetron sputtering [15] and electrophoretic deposition [16]. Subsequently the composite underwent a thermal treatment to modify the grain boundary microstructures and hence to improve the coercivity. Zeng et al [17] have applied Pr-Al-Cu ribbons to cover on the sintered NdFeB magnet surfaces. With Al diffusion into 2:14:1 main phases, the magnet

remanence decreased. Additionally, Pr-Cu alloys with low melting point were implemented to hot-deformed NdFeB magnets by GBDP [18-19,20]. As reported, the remanences of the hot-deformed magnets all decreased a lot due to the nonmagnetic RE-Cu alloy phases formed at the RE-rich grain boundaries. The previous investigations mainly focused on the inorganic compounds i.e. fluoride, hydride and oxide of HRE, and the low melting point HRE-Cu/Al alloys by GBDP. In contrast, we selected light rare earth (LRE) Pr-Zn to improve coercivity without reducing remanence.

In this work, the non-HRE Pr-Zn films were prepared on the NdFeB magnet surfaces by DC magnetron sputtering. The magnetic properties, thermal stability and microstructures of the annealed and Pr/Dy-Zn GBDP magnets were compared. The coercivity enhancement mechanism and thermal stability of diffused magnets were also discussed.

2. Experimental Procedure

2.1 Materials

The commercial as-sintered NdFeB magnet (N38, Ganzhou Fortune Electronic Co. Ltd.) was selected as starting magnets. The magnet was mechanically cut into cuboids about 10 mm×10 mm×4.5 mm (4.5 mm was the alignment of c-axis). Then the surfaces of the cut magnets were ground with abrasive SiC papers from 400 to 2000 grit, and subsequently polished into a light mirror surface. All samples were cleaned cyclically in alkaline, deionized water and ethanol by ultrasonic cleaner, and dried in a vacuum oven. The purities of commercial Pr and Zn targets are 99.95% and 99.99%, respectively.

2.2 Preparation process

It has been demonstrated that diffusion efficiency of the as-sintered NdFeB magnets was much higher than that of the annealed ones [21]. So the as-sintered magnets were selected as original substrate materials. The magnet surfaces were covered by Pr-Zn films via DC-magnetron sputtering system at room temperature. During deposition, the base pressure of the chamber was ~3×10^{-3} Pa and the pressure for sputtering was maintained at 0.9-1.2 Pa. The DC power of the targets was 80-150 W and co-sputtering time was 2 hours. After deposition process, the film-deposited

magnets suffered a thermal diffusing treatment at 600-900 ℃ for 1-11 hours and subsequent annealing treatment at 450-550 ℃ for 2 hours in 5×10^{-3} Pa vacuum. Notably, the magnets after thermal diffusing and following annealing treatment are designated as Pr-Zn GBDP magnet, and all the treated magnets are referred to the optimally thermal treatment ones.

2.3 Characterization methods

The magnetic properties of the magnets at different temperatures were measured by a B-H tracer device (NIM-500C). The magnetic flux losses were measured by rapidly pulling Helmholtz coil method after exposure at different temperatures. The microstructures and compositions of NdFeB magnets were observed by scanning electron microscope (SEM) with an energy dispersive X-ray spectrometer (EDS) (ΣIGMA). The micro-area composition analysis of NdFeB magnets was performed by electron probe micro-analyzer (EPMA) with a wavelength dispersive X-ray spectrometer (WDS) (JXA-8100).

3. Results and Discussion

Figure 1 shows the cross-sectional backscattered SEM image and line-scanned EDS results of Pr-Zn film on the as-sintered NdFeB magnet surface. As exhibited, it is observed that Pr-Zn films are uniformly attached on the magnet surfaces, which suggests the suitability for preparing the films via magnetron sputtering method. The thickness of Pr-Zn films is approximately 5-6 μm. This provides a highly energetic and easily controlled way for GBDP treatment. From the line-scanned EDS results, it is also proved that Pr and Zn elements have been effectively deposited onto the surface of the NdFeB substrate material.

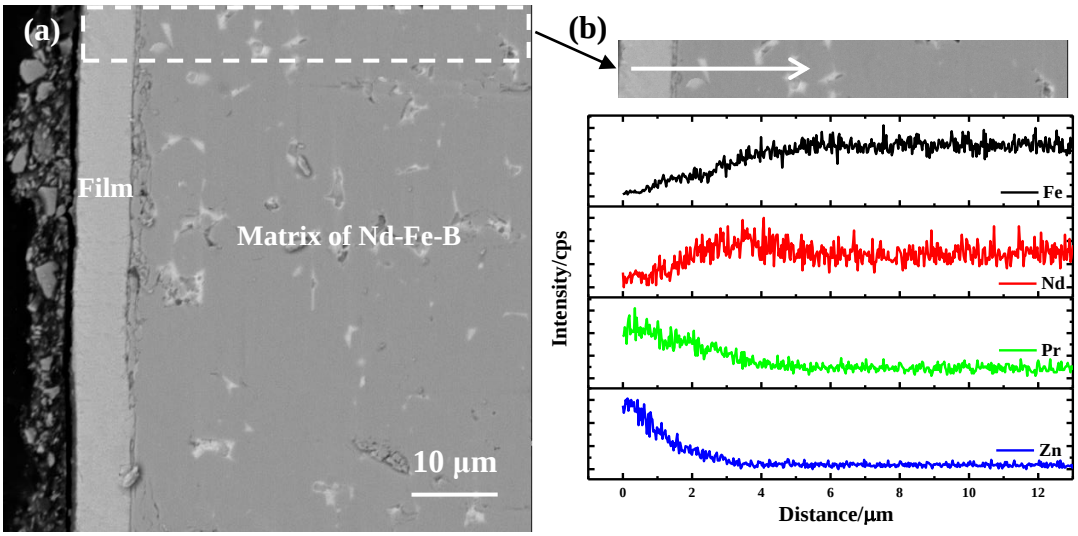

Fig.1 Cross-sectional SEM image and line scanned EDS results of Pr-Zn film on the as-sintered NdFeB magnet surface

The demagnetization curves of different thermal treatment NdFeB magnets along with the corresponding magnetic values are shown in Fig. 2(a) and Table 1. As observed, the coercivity of NdFeB magnet was enhanced significantly after GBDP technique. Its coercivity was 1317.14 kA m^{-1}, higher than 963.96 kA m^{-1} of the as-sintered magnet, with an increment of 36.64%. Meanwhile, the remanence of both magnets stayed invariable at 1.21 T. Notably, the squareness of the demagnetization curves still maintained well, which was only lowered to 97.7% from 98%. Moreover, the coercivities were increased to 1033.21 kA m^{-1} and 1071.58 kA m^{-1} separately by annealing and thermal diffusion treatment, respectively. However, the coercivities have been enhanced strikingly via GBDP treatment. Thus, such approach serves as an efficient way to improve the coercivities of NdFeB magnets without sacrificing the remanence and squareness factor by grain boundary diffusing non-HRE alloys.

Fig. 2(b) shows the demagnetization curves of the annealed and Pr-Zn GBDP magnets at 20, 50, 80, 120 and 180 ℃. The coercivity and saturation magnetization of the annealed and Pr-Zn GBDP magnets were both decreased gradually with increasing the temperature from 20 to 180 ℃. The coercivity of the annealed and Pr-Zn GBDP magnets was deduced to 552.03 kA m^{-1} and 732.16 kA m^{-1} at 80 ℃, respectively. Fig. 2(c) also shows coercivities variation of the annealed and Pr-Zn GBDP magnets at

different temperatures. All coercivities of Pr-Zn GBDP magnets were higher than the annealed one at the same temperature. However, the coercivity differences between two composites were decreased gradually when temperature rises. This can be attributed to that the coercivities are susceptive to high temperatures [25].

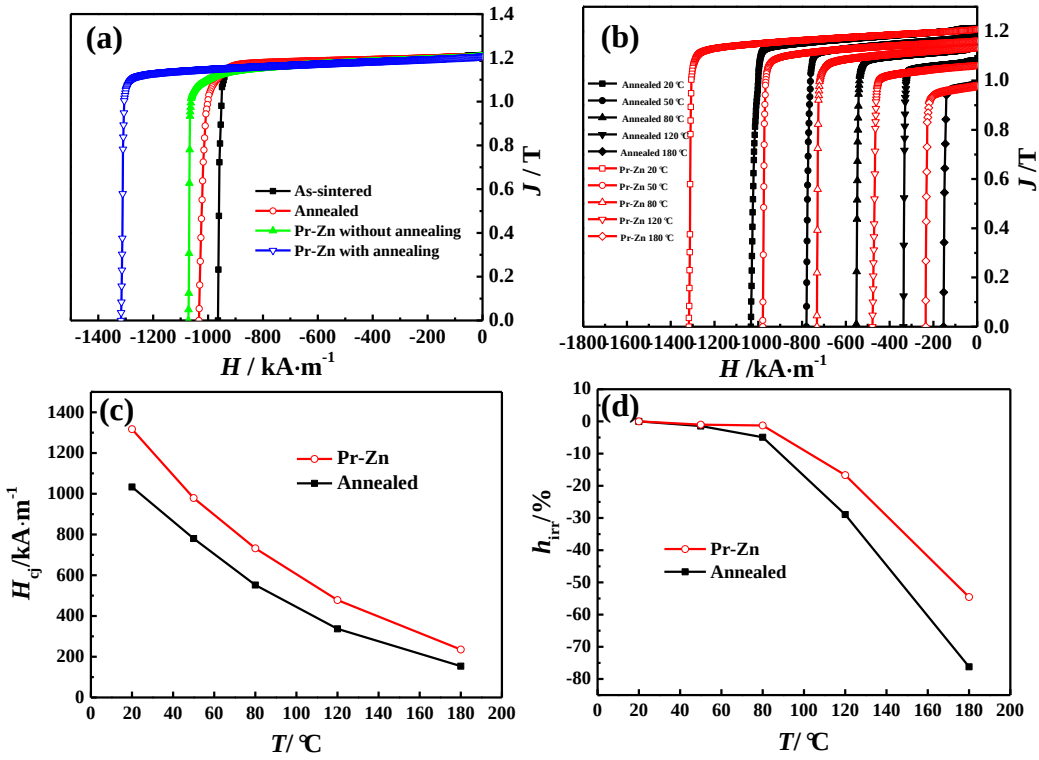

Fig. 2 Magnetic properties of NdFeB magnets: Demagnetization curves of different thermal treatment magnets at room temperature (a), Demagnetization curves of the annealed and Pr-Zn GBDP magnets at 20, 50, 80, 120 and 180 ℃ (b), Coercivity versus temperature curves of the annealed and Pr-Zn GBDP magnets (c), Magnetic flux losses of the annealed and Pr-Zn GBDP magnets exposed at 20, 50, 80, 120 and 180 ℃ for 2 h (d)

Table 1 Magnetic properties of different thermal treatment NdFeB magnets

Samples	H_{cj} (kA·m^{-1})	B_r (T)	$(BH)_{max}$ (kJ·m^{-3})	H_k/H_{cj} (%)
As-sintered	963.96	1.212	280.67	98.00
Annealed	1033.21	1.205	281.94	94.60
Pr-Zn without annealing	1071.58	1.206	275.70	95.10
Pr-Zn with annealing	1317.14	1.208	278.07	97.70

The temperature coefficient of coercivity (β_{Hcj}) is a key factor to NdFeB magnets.

It can be defined as:

$$\beta_{H_{cj}} = \frac{H_{cj}(T) - H_{cj}(T_0)}{H_{cj}(T_0)(T - T_0)} \times 100\% \quad (1)$$

Where T and T_0 refer to an elevated temperature and room temperature, respectively. The temperature coefficient of coercivity from 20 to 120 ℃ was calculated based on the data from Fig. 2(c) and equations (1). The value of β_{Hcj} was improved to -0.6370 %/℃ of Pr-Zn GBDP magnet from -0.6740 %/℃ of the annealed one. The decrement of the absolute value ($|\beta_{Hcj}|$) implies the betterment of thermal stability for the Pr-Zn GBDP magnet.

Furthermore, another important factor of NdFeB magnet in applications is the irreversible magnetic flux loss (h_{irr}). The magnetic flux of NdFeB magnet has severely dropped under long-term high temperature environment. The magnetic fluxes of the both samples were measured by pulling Helmholtz coil method at different temperatures for 2 h. Fig. 2(d) shows the magnetic flux losses of both materials exposed at 20, 50, 80, 120 and 180 ℃ for 2 h. The absolute values of irreversible flux losses both increased with raised temperatures. The magnetic fluxes reduced slowly at 20-80 ℃, but it dropped rapidly at 80-180 ℃ due to the thermal susceptivity of coercivity. The value of $|h_{irr}|$ for the annealed magnet was 28.9% while the other one was 16.7% at 120 ℃ for 2 h. The irreversible flux losses were reduced for the Pr-Zn GBDP magnets. It can be concluded that thermal stability of NdFeB magnets has been remarkably improved after using GBDP treatment.

In order to shed light on the reasons for magnetic property and thermal stability improvements of NdFeB magnets, SEM and EPMA were conducted to measure the microstructures and compositions distribution of the both magnets. Fig. 3 shows SEM backscattered images of the original and Pr-Zn GBDP magnets. They are mainly composed of dark gray $Nd_2Fe_{14}B$ main phases and bright white RE-rich phases. The blurred boundary of main grain phases of the original magnet can be clearly seen from Fig. 3(a), which easily leads to direct contact of the neighboring main phases. This is one of the main reasons for low coercivity of the original magnet. Fig. 3(b) depicts the enhanced amount of thin layer RE-rich grain boundary phases of Pr-Zn GBDP magnet,

as compared to that of the original one. This gives rise to sufficient isolation between main grains, and the enhanced exchange decoupling of the main grains should be responsible for coercivity improvement of NdFeB magnet after GBDP technique.

Moreover, Pr elements on the magnet surface diffuse into magnet interior along liquid grain boundary phases when using GBDP treatment. The concentration of Pr elements at RE-rich phases marked in 2 and 4 is much higher than that of main grains marked in 1 and 3 from the EDS results in Table 2. In terms of Pr-Zn GBDP magnet, most of Pr elements mainly aggregate at the triple junction RE-rich phases, and a small amount of Pr elements form some thin layer RE-rich phases along diffusion channels. The thin layers of RE-rich grain boundary phases are beneficial to the coercivity enhancement for the Pr-Zn GBDP magnet. In addition, some Pr elements diffusing into main grains can also improve the magnet coercivity due to higher magneto-crystalline anisotropy field of $Pr_2Fe_{14}B$ (5970 kA m^{-1}) than that of $Nd_2Fe_{14}B$ (5811 kA m^{-1}) [22].

It can be inferred that the optimized microstructure of RE-rich phases and the enhanced magnetic decoupling of main grains are the main reasons for coercivity improvement of NdFeB magnets after using GBDP treatment. The higher room-temperature coercivity of NdFeB magnets can compensate coercivity losses at high temperatures. Therefore, thermal stability of NdFeB magnets has been improved by GBDP technique.

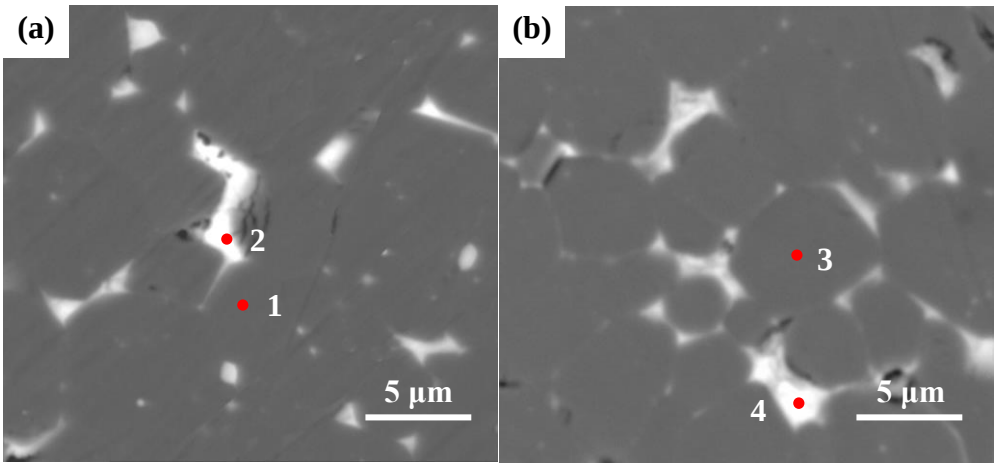

Fig. 3 SEM images of the original and Pr-Zn GBDP magnets

Table 2 EDS results of the magnets marked in Fig. 3 (wt.%)

Main elements	1	2	3	4

O	0.68	6.03	0.82	1.40
Fe	71.35	7.8	70.03	5.23
Pr	5.75	22.32	6.41	33.89
Nd	20.37	60.62	21.11	57.44

Fig. 4 shows the cross-sectional EPMA images of the original and Pr-Zn GBDP magnets at the depth of 0-250 μm. It is clearly seen that Nd elements of both samples are homogeneously distributed, and most of Nd elements are enriched in the RE-rich grain boundaries. Notably, the distribution of Pr elements is more discrete than that Nd elements. It can also be observed that the amount of Pr elements in Pr-Zn GBDP magnet becomes much more than that of the original one. Pr elements of Pr-Zn GBDP magnet possess larger distribution regions compared to the original one seen from Fig. 4(a) and 4(b). Notably, the higher amount of Nd elements in Pr-Zn GBDP magnet is due to the preferential displacement of Pr towards Nd elements of the main grains when diffusing Pr-Zn films into inside of the magnet [17]. The Nd elements replaced by Pr elements supply the contents of Nd in the grain boundary phases. This would optimize the microstructure and compositions of the magnet, leading to improved coercivity based on GBDP process.

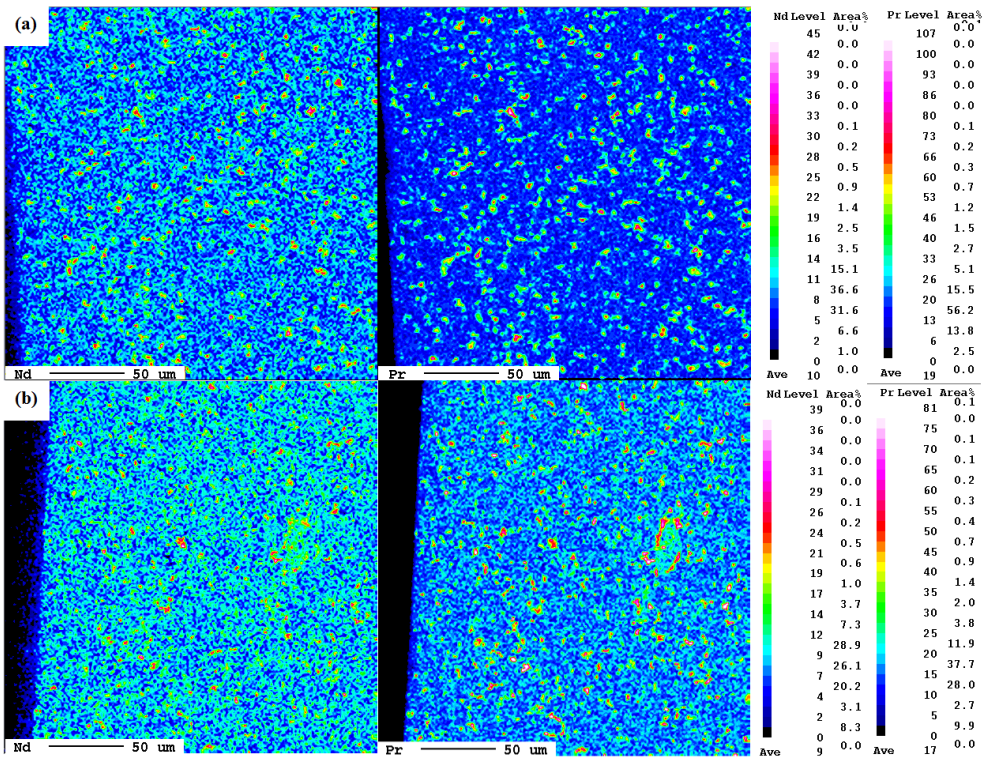

Fig.4 Cross sectional EPMA images of the original and Pr-Zn GBDP magnets at the depth from 0-

250 μm

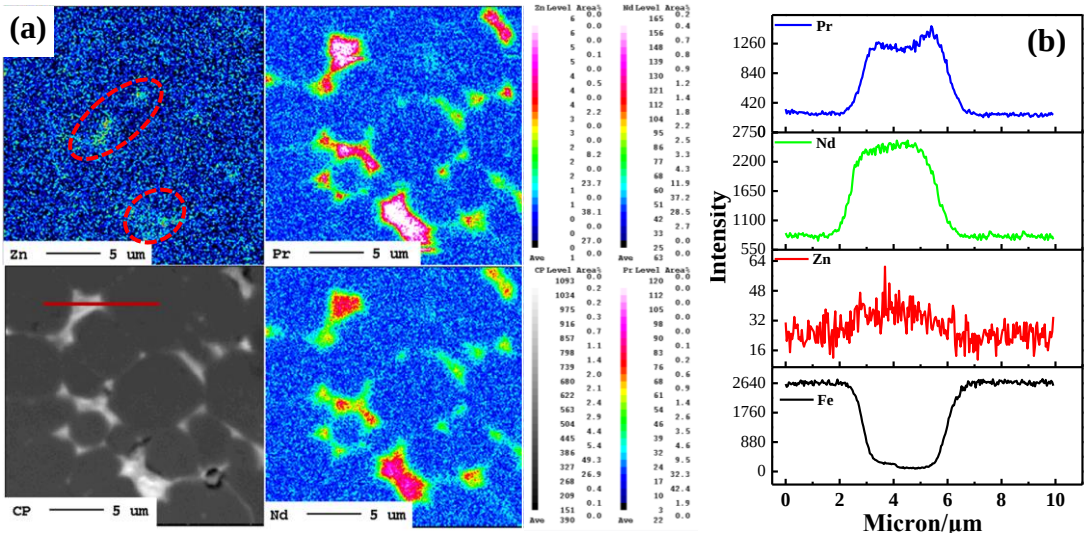

Fig. 5 EPMA and WDS images on the sub-surface of Pr-Zn GBDP magnet

In order to further clarify composition distribution of RE and Zn elements precisely, EPMA images and line scanned WDS results on the sub-surface of Pr-Zn GBDP magnet are shown in Fig.5. It is clearly shown that Pr, Nd and Zn elements mainly enrich in the triple junction RE-rich phases from Fig. 5(a). Due to the easily evaporated Zinc, a small amount of Zn elements are detected in the Zn mapping image. The line-scanned WDS results show that content distributions of Pr and Zn elements are consistent with Nd elements, while opposite to Fe elements in Fig. 5(b) marked in a red line. It is confirmed that the elements mainly diffuse along liquid grain boundary phases and segregate at RE-rich phases. This is attributed to greater atomic diffusion coefficient in the liquid RE-rich phases than that in the solid main phases.

The eutectic reaction of Pr and Zn elements may occur at 576 ℃ based on Pr-Zn binary phase diagram [23]. The RE-rich phases begin to melt into liquid phases since temperature increased to over 655 ℃ [24]. PrZn alloy diffusing into RE-rich phases can reduce the melting point of liquid phases and provide more diffusing channels, which can improve diffusion efficiency of the magnet. As diffusion proceeds, the most part of Pr elements continue to diffuse along the formed liquid phase channels. This would improve the wettability and mobility of RE-rich grain boundary phases and avoid direct contact between the main grains. The amount of thin layer RE-rich grain boundary phases of Pr-Zn GBDP magnet becomes much more than the original one.

Hence, the morphology of RE-rich grain boundary phases is optimized and becomes more continuous and smooth, which can inhibit the nucleation of reverse magnetic domains and improve intrinsic coercivity for the Pr-Zn GBDP magnet.

It is widely known that the coercivity of sintered NdFeB magnets depends on the nucleation of reverse magnetic domains [25]. The coercivity H_{cj} is usually expressed as:

$$\mu_0 H_{cj} = \alpha \mu_0 H_A - N_{eff} M_S \quad (2)$$

Where H_A and M_S refer to the effective anisotropy field and saturation magnetization of $RE_2Fe_{14}B$, respectively. The α represents the microstructural factor, which is related to grain size, grain alignment and some surface defects of grains. N_{eff} refers to the effective demagnetization factor related to grain size, grain shape and the stray field of grain boundaries, etc. The α and N_{eff} are both microstructure sensitivity parameters. The main factors influencing magnetic properties of NdFeB magnets are the magneto-crystalline anisotropy field of $RE_2Fe_{14}B$ and exchange decoupled interaction of main grains resulted from the separation of RE-rich phases.

Fig. 6 shows the demagnetization curves of Pr-Zn and Dy-Zn GBDP magnets. The coercivity of Dy-Zn GBDP magnet was improved to 1711.40 kA m^{-1} from 963.96 kA m^{-1} of the as-sintered one after GBDP treatment, which was 394.26 kA m^{-1} higher than that of Pr-Zn GBDP one. However, the squareness of the curve in Pr-Zn GBDP magnet was 97.70% higher than that of Dy-Zn GBDP one (87.60%). This is due to much higher anisotropy field of $Dy_2Fe_{14}B$ of 11940 kA m^{-1} than that of $Pr_2Fe_{14}B$ and $Nd_2Fe_{14}B$ (5970 kA m^{-1} and 5811 kA m^{-1}, respectively) [22]. The HRE elements prefer to substitute for Nd elements at main phase grain epitaxial layers to form higher anisotropic $(Nd,Dy)_2Fe_{14}B$ phases, so-called the core-shell structure [13]. The magnetic hardening of main phase grain epitaxial layers should take the main responsibility for the great coercivity improvement of Dy-Zn GBDP magnet. In addition, it can lead to microstructure inhomogeneity which is the possible reason for the drop of the squareness for Dy-Zn GBDP magnet. As mentioned above, the optimized RE-rich grain boundary phases, especially the thin layer RE-rich microstructures would enhance magnetic exchange decoupled interaction, which serves as the main reason for the

coercivity increment of Pr-Zn GBDP magnet. Based on the similar composition of diffusion source to the original magnet (PrNd is often used as raw materials in business), microstructure of Pr-Zn GBDP magnet would be more homogeneous than that of Dy-Zn GBDP one. The microstructure homogeneity on the magnet surface plays an important role in maintaining a good squareness of the demagnetization curve. The squareness of Pr-Zn GBDP magnet keeps almost invariably, which can enhance the anti-demagnetization ability of the magnets in high temperature applications.

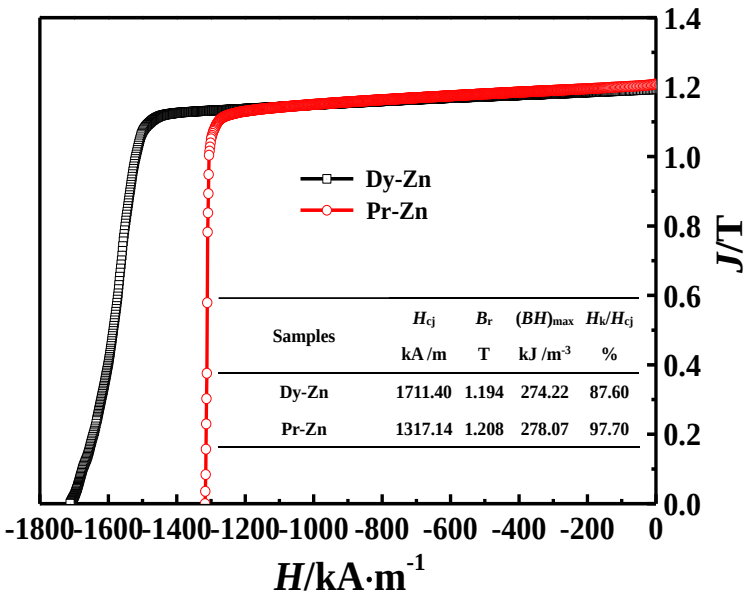

Samples	H_{cj} kA /m	B_r T	$(BH)_{max}$ kJ /m^{-3}	H_k/H_{cj} %
Dy-Zn	1711.40	1.194	274.22	87.60
Pr-Zn	1317.14	1.208	278.07	97.70

Fig. 6 Demagnetization curves of Dy-Zn and Pr-Zn GBDP magnets

Fig. 7 shows the scheme of whole diffusion process for Pr-Zn and Dy-Zn GBDP magnets. In fact, the process of diffusing RE alloys is similar to diffusing RE metals/compounds for NdFeB magnets via using GBDP technique. RE alloys diffuse into the interior of NdFeB magnet along RE-rich grain boundary liquid phases during thermal diffusion process. Comparing with pure RE metals/inorganic compounds, RE alloys can further reduce the melting point of RE-rich liquid phases and increase volume fraction of RE-rich phases which can provide more diffusing channels. Therefore, diffusion efficiency of the magnets has been improved and diffusion temperature and time have been reduced especially for LRE alloys due to its lower melting point than HRE alloys.

In summary, Pr/Dy elements would prefer to substitute for Nd in the epitaxial layer of main phase grains and form $(Nd,Pr/Dy)_2Fe_{14}B$ phases surrounding the main grains

during GBDP. According to the rule of mixtures which can be expressed as $H_A^{eff} = H_A^{Nd} \times \text{Nd at\%} + H_A^{RE} \times \text{RE at\%}$ and RE refers to Pr/Dy($H_A^{Pr} < H_A^{Dy}$) [26], the effective anisotropy field of Pr-Zn diffused magnet is much smaller than that of Dy-Zn diffused one. This is why the coercivity of Pr-Zn GBDP magnet is much lower than that of Dy-Zn GBDP one. Additionally, the coercivity in Fig. 2(a) would be further enhanced due to the optimized grain boundary phase microstructures after the following proper annealing treatment. Thus, the coercivities of Pr/Dy-Zn GBDP magnet mainly depend on the effective anisotropy field of Pr/Dy-rich shells surrounding main grain cores and the optimization of RE-rich grain boundary phase microstructures. In other words, the magnetic hardening of epitaxial layers and exchange decoupled interactions of main grains are the key factors to influence intrinsic coercivity of NdFeB magnets after using GBDP technique.

Fig.7 Scheme of the whole diffusion process for Pr-Zn and Dy-Zn GBDP magnets

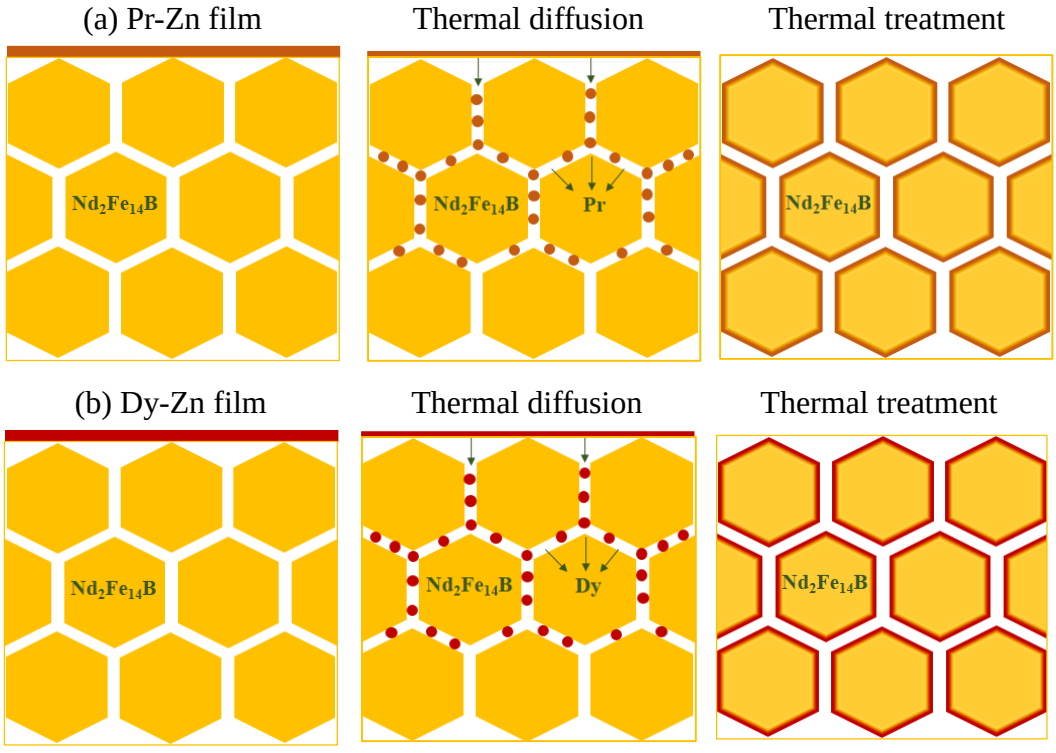

4. Conclusions

The magnetic properties, thermal stability and microstructure of sintered NdFeB magnets with diffusing Pr-Zn films via magnetron sputtering technique are investigated systematically in the work. The conclusions are drawn as follows:

1. The intrinsic coercivity of Pr-Zn GBDP magnets was improved from 963.96 kA $\cdot m^{-1}$ to 1317.14 kA $\cdot m^{-1}$ without any reduction in remanence and the squareness of the demagnetization curve remained well due to the homogeneous microstructures on the magnet surface after using GBDP treatment.

2. The thermal stability of Pr-Zn GBDP magnets is improved after using GBDP treatment. The temperature coefficient of the coercivity was improved from -0.6740 %/℃ to -0.6370 %/℃ in the temperature range of 20-120 ℃. The irreversible flux losses were reduced from 28.9% to 16.7% at 120 ℃ for 2 h.

3. The magnetic hardening layers of $(Nd,RE)_2Fe_{14}B$ around the outer region of main grains and the optimization of RE-rich grain boundary phases should take the main responsibilities for the enhancement of the coercivity and thermal stability via performing GBDP technique.

Acknowledgments

This work was partially supported by the National Natural Science Foundation of China (51561009), the Higher School Science and Technology Landing Project of Jiangxi Province (KJLD14043), the Youth Science Foundation Project of Jiangxi Province (20151BAB216005) and the Doctoral Start-up Foundation of Jiangxi University of Science and Technology (3401223391). Dr. Li also thanks the China Scholarship Council (CSC No. 201703000006) for funding to visit Nanyang Technological University, Singapore.

References

[1] M. Sagawa, S. Fujimura, N. Togawa, H. Yamamoto, and Y. Matsuura, New material for permanent magnets on a base of Nd and Fe (invited), J. Appl. Phys. **55** (1984) 2083-2087.
[2] O. Gutfleisch, M.A. Willard, E. Brück, C.H. Chen, S. G. Sankar , and J. P. Liu, Magnetic Materials and Devices for the 21st Century: Stronger , Lighter , and More Energy Efficient, Adv. Mater. **23** (2011) 821-842.
[3] R. Sun, J. Zheng, B. Zheng, N. Qian, J. Li, Z. Deng, New magnetic rails with double-layer Halbach structure by employing NdFeB and ferrite magnets for HTS maglev, J. Magn. Magn. Mater. 445 (2018) 44–48.
[4] Y. Matsuura, Recent development of Nd – Fe – B sintered magnets and their applications, J. Magn. Magn. Mater. 303 (2006) 344–347.
[5] G. Bai, R.W. Gao, Y. Sun, G.B. Han, B. Wang, Study of high-coercivity sintered NdFeB magnets, J. Magn. Magn. Mater. **308** (2007) 20–23.
[6] Z.H. Hu, F.Z. Lian, M.G. Zhu, W. Li, Effect of Tb on the intrinsic coercivity and impact toughness of sintered Nd-Dy-Fe-B magnets, J. Magn. Magn. Mater. **320** (2008) 1735–1738.
[7] S. Z. Zhou, and Q. F. Dong, Supermagnets: Rare-Earth & Iron System Permanent Magnet, Metallurgical Industry Press, China, 2004, p.29.
[8] Z.H. Hu, D.W. Ma, H.J. Qu, J.Q. Zhao, C. Luo, H.J. Wang, Effect of Dy Addition on the Magnetic and Mechanical Properties of Sintered Nd-Fe-B Magnets Prepared by Double-Alloy Powder Mixed Method, IEEE Trans. Magn. **51**(11) (2015) 2104203.
[9] K.T. Park, K. Hiraga, M. Sagawa, Effect of metal-coating and consecutive heat treatment on coercivity of thin Nd-Fe-B sintered magnets, in: Proceedings of the 16th Workshop on Rare-earth Magnets and Their Applications, Sendai, 2000, 257-264.
[10] H. Nakamura, K. Hirota, M. Shimao, T. Minowa, M. Honshima, Magnetic properties of extremely small Nd-Fe-B sintered magnets, IEEE Trans. Magn. **41** (2005) 3844–3846.
[11] T. Ma, X. Wang, X. Liu, C. Wu, M. Yan, Coercivity enhancements of Nd-Fe-B sintered magnets by diffusing DyH_x along different axes, J. Phys. D: Appl. Phys. **48** (2015) 215001.
[12] T.H. Kim, S.R. Lee, H.J. Kim, M.W. Lee, T.S. Jang, Simultaneous application of Dy-X (X = F or H) powder doping and dip-coating processes to Nd-Fe-B sintered magnets, Acta Mater. **93** (2015) 95–104.
[13] H. Sepehri-Amin, T. Ohkubo, K. Hono, The mechanism of coercivity enhancement by the grain boundary diffusion process of Nd-Fe-B sintered magnets, Acta Mater. **61** (2013) 1982–1990.
[14] M. Tang, X. Bao, K. Lu, L. Sun, J. Li, X. Gao, Boundary structure modification and magnetic properties enhancement of Nd-Fe-B sintered magnets by diffusing (PrDy)-Cu alloy, Scripta Mater. **117** (2016) 60–63.
[15] B. Wu, X. Ding, Q. Zhang, L. Yang, B. Zheng, F. Hu, Z. Song, The dual trend of diffusion of heavy rare earth elements during the grain boundary diffusion process for sintered Nd-Fe-B magnets, Scripta Mater. **148** (2018) 29–32.
[16] X. Cao, L. Chen, S. Guo, R. Chen, G. Yan, A. Yan, Impact of TbF_3 diffusion on coercivity and microstructure in sintered Nd-Fe-B magnets by electrophoretic deposition, Scripta Mater. **116** (2016) 40–43.
[17] H. Zeng, Z. Liu, W. Li, J. Zhang, L. Zhao, X. Zhong, H. Yu, B. Guo, Significantly enhancing the coercivity of NdFeB magnets by ternary Pr-Al-Cu alloys diffusion and understanding the elements diffusion behavior, J. Magn. Magn. Mater. **471** (2019) 97–104.
[18] X. Tang, R. Chen, W. Yin, C. Jin, D. Lee, A. Yan, The magnetization behavior and open recoil loops of hot-deformed Nd-Fe-B magnets infiltrated by low melting point PrNd-Cu alloys, Appl. Phys. Lett. **107** (2015) 2–7.
[19] H. Sepehri-Amin, L. Liu, T. Ohkubo, M. Yano, T. Shoji, A. Kato, T. Schrefl, K. Hono, Microstructure and temperature dependent of coercivity of hot-deformed Nd-Fe-B magnets diffusion processed with Pr-Cu alloy, Acta Mater. **99** (2015) 297–306.
[20] Z. Wang, J. Zhang, J. Wang, J. Ju, R. Chen, X. Tang, W. Yin, D. Lee, A. Yan, Coercivity improvement of hot-deformed Nd–Fe–B magnets by stress-induced Pr–Cu eutectic diffusion, Acta Mater. **156** (2018) 136–145.
[21] J. J. Li, C. J. Guo, T. J. Zhou, X. F. Rao, H. J. Zhou, and B. Yang, Magnetic Properties and Dysprosium Infiltration of Sintered Nd-Fe-B Magnets by Magnetron Sputtering, Mater. Rev. **31** (2017) 17-20.

[22] J.F. Herbst, $R_2Fe_{14}B$ materials: Intrinsic properties and technological aspects, Rev. Mod. Phys. **63** (1991) 819-898.
[23] J. T. Mason and P. Chiotti, Phase relations and crystallographic data for the Pr-Zn system, Metall. Trans. **1** (1970) 2119-2123.
[24] L. Liang, T. Ma, P. Zhang, J. Jin, M. Yan, Coercivity enhancement of NdFeB sintered magnets by low melting point $Dy_{32.5}Fe_{62}Cu_{5.5}$ alloy modification, J. Magn. Magn. Mater. **355** (2014) 131-135.
[25] K. Hono, H. Sepehri-Amin, Strategy for high-coercivity Nd-Fe-B magnets, Scripta Mater. **67** (2012) 530–535.
[26] R. Ramesh, A microstructure based magnetization reversal model in sintered Fe-Nd-B magnets, J. Appl. Phys. **68** (1990) 5767-5771.